# Synthesis, Characterization and Evaluation of Urethane Co-Oligomers Containing Pendant Fluoroalkyl Ether Groups

Jereme R. Doss[1], Michelle H. Shanahan[1], Christopher J. Wohl[2] and John W. Connell[2]

[1]National Institute of Aerospace, Hampton, VA 23666-6147, United States

[2] Advanced Materials and Processing Branch, NASA Langley Research Center, Hampton, VA 23681-2199, United States

Abstract

Coatings with the ability to minimize adhesion of insect residue and other debris are of great interest for future aircraft. These aircraft will exhibit increased fuel efficiency by maintaining natural laminar flow over greater wing chord distances. Successful coatings will mitigate the adhesion of debris on laminar flow surfaces that could cause a premature transition to turbulent flow. The use of surface modifying agents (SMA) that thermodynamically orient towards the air side of a coating can provide specific surface chemistry that may lead to a reduction of contaminate adhesion. Aluminum surfaces coated with urethane co-oligomers containing various amounts of pendant fluoroalky ether groups were prepared, characterized and tested for their abhesive properties. The coated surfaces were subjected to controlled impacts with wingless fruit flies (*drosophila melanogaster*) using both a benchtop wind tunnel and a larger-scaled wind tunnel test facility. Insect impacts were recorded and analyzed using high-speed digital photography and the remaining residues characterized using optical surface profilometry and compared to that of an aluminum control. It was determined that using fluorinated oligomers to chemically modify

coating surfaces altered the adhesion properties relative to the adhesion of insect residues to the surface.

## INTRODUCTION

As part of an effort to develop coatings to minimize the adhesion of undesirable substances to aerospace surfaces, research has been conducted on the synthesis, characterization and evaluation of urethane based coatings containing surface modifying agents (SMAs). NASA has several on-going and planned future projects with a need for surface engineered materials that mitigate or minimize the adhesion of a variety of species in diverse, and extreme environments. For example, preventing dust particles that might be encountered in extraterrestrial environments from accumulating on a solar array [1], ice and water droplets from accumulating during aircraft flight [2], or preventing insect residue from adhering to future aircraft surfaces thereby disrupting laminar flow, increasing drag and reducing fuel efficiency. [3] A number of effective techniques to modify the surface chemistry of polymeric materials have been investigated including chemical or physical vapor deposition [4], self-assembled monolayers [5], surface-confined chemical reactions [6], block co-polymers [7], SMAs [8] and polymer brush growth. [9] [10] The approach described herein uses SMAs in the form of commercially available hydroxyl terminated oxetane-derived oligomers containing pendant fluoroalkyl groups that are co-reacted with toluene diisocyanate and 1,4-butanediol to form controlled molecular weight random co-oligomers.

SMAs are thermodynamically drawn to the air side surface of a material enabling controlled surface chemical modification with minimal SMA incorporation. [9] [11] This alters the surface energy which can dramatically affect properties such as wettability and adhesion, however the bulk properties of the base polymer are largely unchanged because effective SMA

loading levels are typically less than 1% (w/w). [12] Fluorine and silicon containing species are well known to migrate to the air side of polymeric based coatings. [13] In fact, in many applications where adhesive bonding is important, great lengths are often employed to avoid contamination by silicon and fluorine containing species due to their known difficulty in forming adhesive bonds. Of the two, fluorine containing species have a greater proclivity for surface migration than silicon containing species and have been demonstrated to undergo surface migration when incorporated into a variety of polymer types including polyesters [14], polyurethanes, polyacrylates, polydimethyl siloxane and polyimides. [15]

Polyurethanes have an excellent combination of physical and mechanical properties that make them useful in a broad array of applications. [16] A number of studies involving structure property relationships of polyurethanes have been reported and the topic reviewed. [17] Fluorine containing diols have been used in polyurethane synthesis to create polymeric films with low surface energy. For example, Tang et al. [18] reported polyurethanes modified with 5% of a fluorinated diol that exhibited water surface wetting characteristics comparable to that of a fully fluorinated polymer, e.g. Teflon®, with no measureable loss of bulk properties. However, a complete understanding and concomitant ability to prevent adhesion of complex, active and dynamic chemical systems such as those encountered with biological species remains a significant challenge. The modification of surface energy alone has proven to be insufficient to prevent such materials from adhering to polymeric surfaces. Other approaches have used SMAs to ferry other chemically active species to a material surface which otherwise would not spontaneously surface migrate. [19]

In this work, the synthesis of controlled molecular weight urethane co-oligomers with various amounts of fluorinated oligomeric diols is presented. The materials were characterized for

surface properties, and spray coated onto aluminum substrates and tested for their ability to prevent insect residue from adhering to the coating surface in a benchtop wind tunnel and a larger-scaled wind tunnel test facility.

## EXPERIMENTAL

**Materials and Methods**. Hydroxyl-terminated PolyFox-656 (PF-656) was purchased from Omnova Solutions and used as received. 1,4-Butandiol (BD) was obtained from Sigma Aldrich and dried for 72 hours over 3Å molecular sieves prior to use. 2,4-Toluene diisocyanate (TDI) from Sigma Aldrich was used as received. The catalyst dibutlytin dilaurate was used as received from Sigma Aldrich. Anhydrous dimethylformamide (DMF) was purchased from Sigma Aldrich and stored over 3Å molecular sieves and filtered using a fritted glass funnel prior to use. Methyl ethyl ketone (MEK) was used as received. $^{1}$H NMR spectra were recorded on a Bruker (Avance 300) Multinuclear Spectrometer operating at 300.152 MHz. The spectra were collected in either $CDCl_3$ or d-DMSO. Polymer films were spray coated from 8% w/w solutions in MEK onto aluminum panels [Al 1100, 3 mil (76.2 μm) thickness] and cured in an oven at 120°C for 2 hours. Prior to coating, the Al panels were wiped with isopropanol. Energy-dispersive X-ray spectroscopy (EDS) studies were conducted using a Thermo Scientific Noran System 7 X-Ray microanalysis system attached to a Hitachi S-5200 field emission scanning electron microscope (SEM). Samples were sputtered with a thin layer (~3 nm) of Au/Pd prior to analysis. The acceleration voltage during the analysis was 10 kV. The EDS spectral acquirement and mapping were both conducted at Rate 5 and 7 as set by the instrument software, which has a maximal throughput of 227000 cps and 417600 cps, respectively, for 30 frames at 10 s/f.

**Urethane Co-Oligomer Synthesis.** Using the general procedure outlined in this section, controlled molecular weight (5000 g/mol) random urethane co-oligomers were prepared by reacting 2,4-toluene diisocyanate (TDI) with various combinations of the BD and PF-656 (Table 1) . The diol content in the NCO/OH molar ratio was always in excess to control the molecular weight (~5000g/mole) and to minimize the presence of reactive isocyanate end groups. In a flame dried 3-necked round bottomed flask equipped with a mechanical stirrer, the diols were added along with DMF. Dibutyltin dilaurate was added to the flask as the catalyst at 1 wt% solids. The flask was stirred and heated to 75°C. Upon heating, the diols dissolved in the DMF to form a light yellow solution. The diisocyanate was added drop-wise over 20 minutes while maintaining the temperature around 75°C. The reactions were carried out at 20 wt % solids under a nitrogen atmosphere over about a 16 hr period, resulting in a colorless solution with a moderate increase in solution viscosity. The reaction was then cooled to room temperature and precipitated in deionized water with vigorous stirring, filtered using a fritted glass funnel, washed multiple times in water and dried under vacuum at 80°C overnight. The white powders were obtained in near quantitative yields. The urethane co-oligomer was characterized by DSC, FTIR, and $H^1$NMR.

Table 1. Percentage of Hard Segment and Soft Segment Content in Urethanes

| Oligomer | Mole Percent Hard Segment | Mole Percent Soft Segment |
|---|---|---|
| Urethane 0 | 100 | 0 |
| Urethane 1 | 99 | 1 |
| Urethane 5 | 95 | 5 |
| Urethane 10 | 90 | 10 |

| | | |
|---|---|---|
| Urethane 20 | 80 | 20 |
| Urethane 30 | 70 | 30 |
| Urethane 100 | 0 | 100 |

**Differential Scanning Calorimetry**. Differential scanning calorimetry (DSC) data were obtained from a Seteram 131 system under a nitrogen atmosphere at a scan rate of 20°C/min. A standard heat/cool/heat profile was used in running the samples. Heating the urethanes above their transition temperatures and cooling at a controlled rate erased the previous thermal history of the urethanes. This allows the second heat to evaluate the intrinsic properties of the urethanes. [20] The samples were initially heated to 200°C and then cooled from 200° to -30°C and heated at 20°C/min to 200°C. Glass transition data were determined during the second heating cycle.

**Fabrication of Coatings.** Powders of the urethane co-oligomer were dissolved in MEK at a concentration of about 8% (w/w) solids and used to prepare coatings by spraying the solutions onto a pre-cleaned Al substrate. The coatings were allowed to air dry in a low humidity chamber. The coatings were characterized by contact angle goniometry and subsequently subjected to fruit fly impact tests in both a benchtop wind tunnel and a larger-scaled wind tunnel test facility.

**Contact Angle Goniometry (CAG).** Water contact angle data were collected using a First Ten Angstroms FTA 1000B contact angle goniometer. Contact angle measurements of 8 μL water droplets were taken while tilting the axis from 0° to 60°. Prior to the experiment, interfacial tension measurements of the suspended water drops were taken to verify water purity and precision of the focused image. Contact angles were determined by drop shape analysis. For all surfaces, contact angles presented are the average of a minimum of three droplets.

**Benchtop Wind Tunnel.** A small scale wind tunnel test was used as a means of screening coatings for their potential to reduce the adhesion of fruit fly residue. An untreated Al panel was used as the control in order to compare insect residue heights and aerial coverage. An insect delivery device was utilized to propel the fruit fly at velocities representative of aircraft takeoff speeds. The device was custom-built and constructed from a VACCON HIGHVAC HVP series 300-Venturi vacuum pump that was modified with an extended delivery nozzle to enable accurate positioning of the insect impact site. [21] Testing was conducted at ambient temperature (approximately 25°C) and about 50- 60% relative humidity. For each event, the airflow was turned on prior to feeding the insect into the insertion port. The suction force rapidly propelled the insect from the delivery port for impact on the test surface. High-speed photography was obtained during impact events using a Vision Research Phantom 12 camera at a speed of 50,000 frames per second.

Prior to each test, velocity measurements were obtained from high-speed photography of the insect trajectory against a 6 cm grid with 0.5 cm graduations. The air pressure was approximately 620 MPa. Insect velocities were determined by dividing the distance by the time, determined from the frame count, required for the insect to traverse the set distance. The velocities were determined to be 234 ± 29 kilometers per hour (kph); well above the requisite for rupture of a fruit fly exoskeleton which is approximately 50 kph. [22]

**Basic Aerodynamic Research Tunnel (BART) Tests.** The BART is a subsonic, atmospheric wind tunnel used to investigate the fundamental characteristics of complex flow fields and to acquire detailed data for the development and validation of computational fluid dynamics (CFD) models and methods. The tunnel has a closed test section that is 0.711 m high, 1.016 m wide, and 3.048 m deep. The free stream velocity was set to 201 km/h and the airfoil (NACA 0015) was

oriented at an angle of attack of 8° to achieve a Reynolds number of 1-2 x $10^6$. More details about the BART facility can be found in references [23] and [24].

**Optical Profilometry.** Insect residue heights were characterized using a FRT of America optical surface profilometer (Microprof 100). Data were collected over the entire region containing visible insect residue at a resolution of 5 μm between data points and 40 μm line to line. Several processing steps were performed on the collected topographical data including: segmentation to remove false zero readings, fitting the baseline to a second-order polynomial, and masking any edge and surface defects. Areal coverage was determined using grain analysis that identified and summed all features above the lowest permissible data plane, typically 8-15 μm, as individual grains. The data plane threshold above the established baseline was necessary to sufficiently separate insect residue features from substrate anomalies.

## RESULTS AND DISCUSSION

**Urethane Characterization.** DSC was measured on powder samples of the urethane co-oligomers. By DSC, the hard segment (Figure 1a) content of the oligomers, consisting of TDI and BD, exhibited glass transition temperatures ($T_g$s) between 80 and 100°C. The soft segment content, composed of TDI and PF-656 (Figure 1b) exhibited $T_g$s between -6 and 3°C. As a control, a urethane oligomer was prepared from TDI and BD (Urethane-0) at a calculated molecular weight of 5000 g/mole. By DSC, this material exhibited a strong transition at 94°C and a much weaker transition at 142°C (Table 2.). [25] In accordance with previous studies, the weaker transition is indicative of the presence of 2,6,-touluene diisocyanate coupled with BD within the oligomer chains. In the case of the urethane co-oligomers containing the SMA, this weaker transition was not detected. A relatively low $T_g$ (below room temperature) was observed for two of the co-

oligomers containing the soft SMA segment (Figure 1b). Being that the soft segment has a fairly large molecular weight when compared to the hard segment, it is not surprising that the soft segment exhibits a separate and low $T_g$ even at low mole percent content. Depending on the orientation within the oligomer, the soft segment seems to form its own phase and disrupts the order and alignment of the hard segment, causing a decrease in the $T_g$. This may have resulted in phase separation that resulted in the hard segment producing a $T_g$ similar the the $T_g$ of the urethane without any SMA content. Interestingly, Urethane-30, containing 30% of PF-656 exhibited a higher $T_g$ for the hard segment than Urethane-10 which contained 10% of PF-656. It might be expected that the $T_g$ would decrease with the increase of soft segment PF-656 content. However, due to the random nature of these urethane co-oligomers, there is most likely variability in the hard block lengths and the sequential arrangement of the hard and soft blocks. No melting endotherms were observed for any of the urethanes which is consistent with the fact that crystalline phases have not been identified in fluoro containing urethane polymers. [26] The SMA used in this study has significant molecular flexibility and pendent side chains and thus would be expected to disrupt any tendency for the co-oligomer to crystallize.

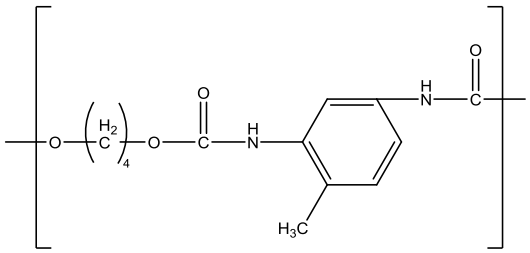

a. Hard Segment

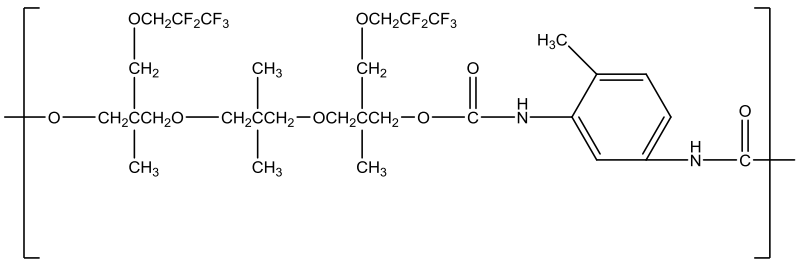

b. Soft Segement

Figure 1. Hard Segment and Soft Segment Structure

Table 2. Thermal Characterization of Urethanes

| Sample | Soft Segment Percentage | $T_g$s, °C | |
|---|---|---|---|
| | | Hard Segment | Soft Segment |
| Urethane-0 | 0 | 94, 142 | ND |
| Urethane-1 | 1 | 88 | ND |
| Urethane-5 | 5 | 85 | 1.71 |
| Urethane-10 | 10 | 87 | -7 |
| Urethane-20 | 20 | 86 | ND |
| Urethane-30 | 30 | 94 | ND |
| Urethane-100 | 100 | ND | 1 |

ND=not detected

**FTIR-ATR.** FTIR-ATR spectra were obtained on the urethane powders and showed broad prominent absorbance bands from the 990-1200 $cm^{-1}$ region which can be assigned to $CF_2$, $CF_3$, and/or C-O stretching. Fluorinated side chains on the co-oligomers that contain PF-656 exhibited absorption peaks at ~1100 $cm^{-1}$. A sharp absorbance peak was observed at 1600 $cm^{-1}$ indicative of the benzene aromatic ring associated with the TDI within the oligomers. The peak at ~1696 $cm^{-1}$ was assigned to the C=O stretching within a primary amide and the NH band appeared around 3300 $cm^{-1}$. Peaks between 1475 $cm^{-1}$ and 1525 $cm^{-1}$ represented the secondary amides

throughout the urethane backbone. Absorptions associated with the ether groups appeared at ~1190 $cm^{-1}$ and ~1050 $cm^{-1}$.

**Fabrication of Urethane Coatings.** Coatings of the various urethanes were prepared using a commercial air brush spraying device. Solutions of the oligomers in MEK were sprayed onto Al 1100 substrates of various sizes and subsequently air dried in a low humidity chamber. The coated samples were subsequently characterized using CAG, and then subjected to fruit fly impact tests. Although no specific control was utilized, the average coating thickness, as determined by a CheckLine DCN-3000FX Coating Thickness Gauge, was 0.16mm.

**Contact Angle Goniometry.** Water contact angle measurements were conducted on the samples prepared as described above and the advancing water contact angle data are presented in Figure 2. The sample containing the highest amount of the SMA (Urethane 100) exhibited the highest water contact angle (~120°), and the sample containing no SMA (Urethane 0) had the lowest (98°). Research has shown that copolymers with blocks containing highly fluorinated side chains exhibit hydrophobicity when in contact with air. [27] The sample containing 1% SMA exhibited a water contact angle of ~100°, and the samples containing 5, 10 and 20% SMA all were around 109°. The water contact angle increased to 113° when the oligomer contained 30% SMA. The increase in the water contact angles reflects the increase in hydrophobicity as the fluorine content increases.

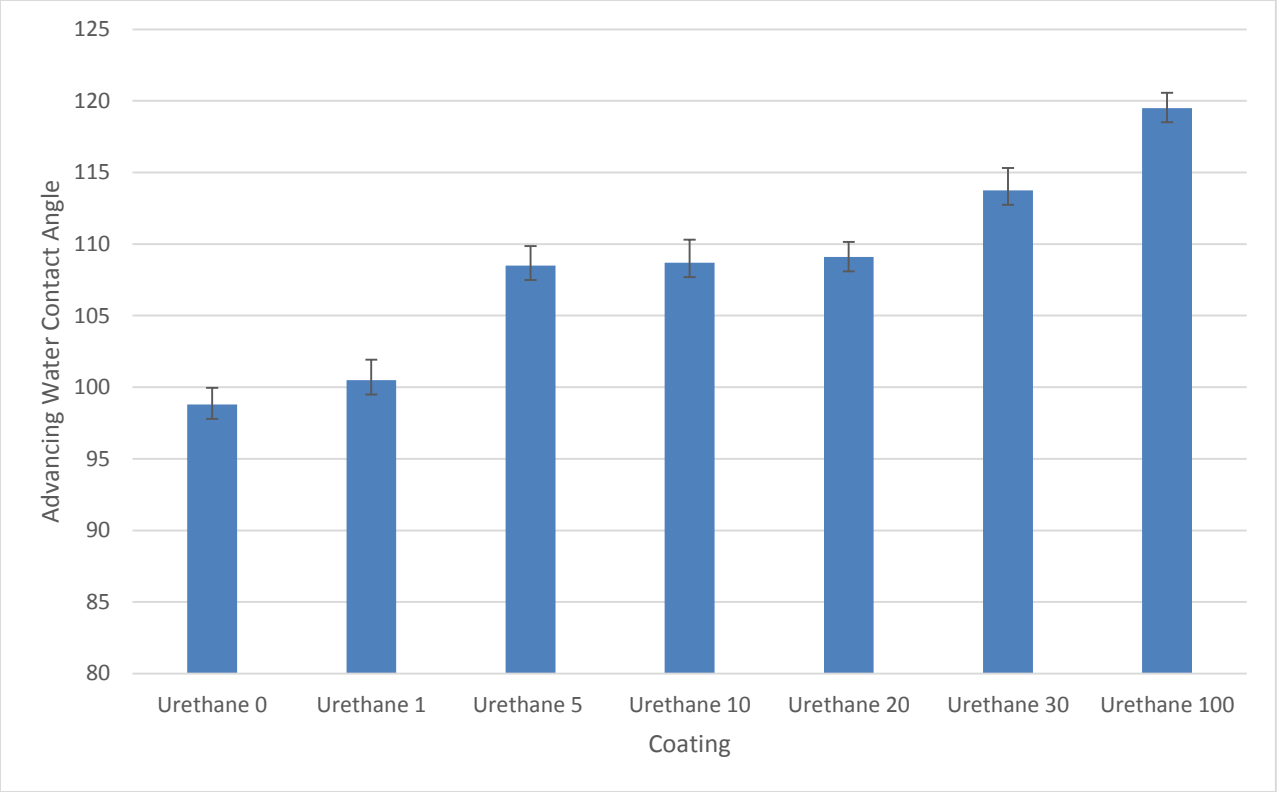


Figure 2. Advancing Water Contact Angle Of The Urethane Co-Oligomers

**Scanning Electron Microscope and Energy Dispersive Spectroscopy.** Investigating the surface of the coatings using a scanning electron microscope (SEM) showed no interesting morphology. No pronounced surface roughness was observed that could be attributed to phase segregation between the hard and soft segments. Energy dispersive spectroscopy (EDS) was used to determine fluorine atoms distribution on the coating surface and was compared to theoretical content in the urethanes (Table 3). Penetration depths for the EDS are on the order of one micron. [28] While the theoretical fluorine content for Urethanes 10 and 20 are both below 10%, the measured surface fluorine content is above 30% for both of the urethanes. As expected, as the SMA content increased in the oligomer, the amount of fluorine at the surface increased indicating preferential migration of the soft segment towards the surface. These results correlate well with the water contact angle measurements.

The decrease in nitrogen content as the fluorine content increased is also indicative of soft segment surface migration. The nitrogen content is derived from both the hard and soft segment via the diol/diisocyanate linkage. As the soft segments migrates, the TDI, which contains the majority of the nitrogen content, is displaced away from the surface. The soft segment has significant molecular weight and mobility compared to the hard segment, consequently it can more readily oriented itself near the surface and displace the hard segment.

In the case of Urethane-100, the increased SMA content led to an exceptionally high fluorine surface content and minimal hard segment surface population as evidenced by the lack of nitrogen detected. The same can be said for the surface oxygen content. As the fluorine content increases, the visible oxygen content decreases as well.

Table 3. Elemental Content of the Urethane Co-Oligomers from EDS Analysis

| Coating | Surface % Carbon | Surface %Nitrogen | Surface % Oxygen | Surface % Fluorine | Theoretical Fluorine Content % |
|---|---|---|---|---|---|
| Urethane-0 | 18 | 21 | 54 | 0 | 0 |
| Urethane-10 | 18 | 20 | 31 | 31 | 3 |
| Urethane-20 | 18 | 12 | 25 | 40 | 7 |
| Urethane-100 | 29 | 0 | 20 | 49 | 35 |

**Benchtop Wind Tunnel Tests.** A benchtop wind tunnel was used as the first screening tool to assess the ability of the coating to resist or minimize adhesion of insect residue. Coated samples were impacted with fruit flies followed by measurement of the residue areal coverage and height using an optical profilometer and compared to those of an uncoated aluminum panel tested under the same conditions. The measurements consist of an averaging of at least three impact residues per test specimen. Only data from insects that were completely intact prior to impact were used in this study. To ensure the insects were whole prior to impact, each test was recorded with a

Vision Research Phantom 1610 high speed video camera. The design of the benchtop wind tunnel allows only one insect to be launched at the coating at a time. Additionally, the majority of the insect collisions are direct hits to the surface of the coating, and do not reflect the true variation of strikes that can occur on airplane wings such as glancing. Thus, these experiments represent a worst-case scenario regarding the amount of insect residue that could be accreted from a single strike. Plots of the average insect residue height and areal coverage for the coatings tested in the benchtop wind tunnel are presented in Figure 3. Due to the nature of this screening test and variables involved, there is a significant amount of error in the data as indicated by the breadth of the errors bars.

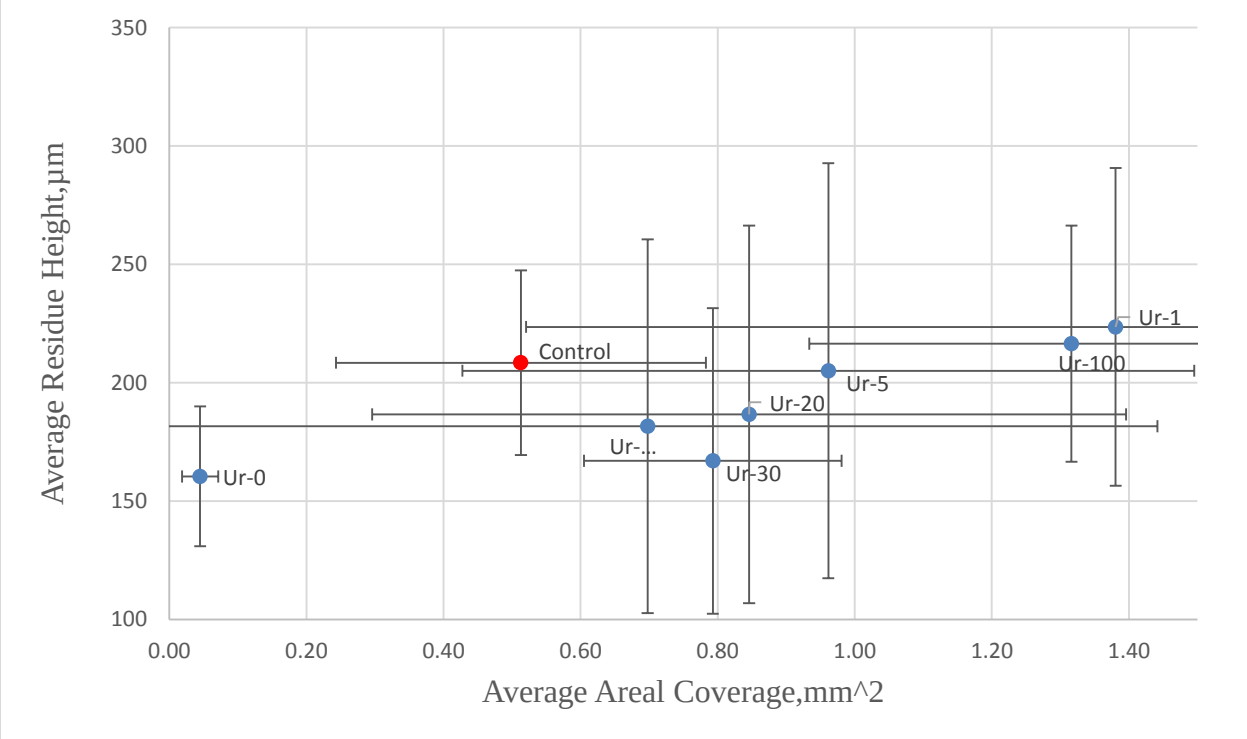


Figure 3. Scatter Plot Of Co-Oligomer Coatings Tested In Benchtop Wind Tunnel

There is significant scatter in the data, which makes comparing residue height and areal coverage difficult, and thus makes interpretation of the results problematic. Regardless, some relationships

can be derived from the results. A comparison of the urethane oligomers containing the SMA with insect residue height and areal coverage individually, shows that as the fluorine content decreased, the insect residue height resulting from the insect impact increased. In the small scale wind tunnel test, Urethane-0, which has no SMA content, had both the lowest residue height and areal coverage of all the coatings tested. Urethane-1 and Urethane-100, which correspond to the urethane oligomers with 1% SMA content and 100% SMA content, respectively, are the only two surfaces that have a higher average insect residue height than that of the control (Figure 4a), . Urethane-0 was the only coating to exhibit a lower average areal coverage than the control (Figure 4b).

There was minimal change in the insect areal coverage Urethanes-1 which had the lowest SMA content and Urethane-100, which had the largest amount of SMA content. Increasing the SMA content from 10 percent (Urethane-10) to 20 percent (Urethane-20) resulted in an increase in both residue height and areal coverage. Urethane-0 had one of the lower contact angles and presumably higher surface energy, yet it had the lowest areal coverage and a residue height similar to Urethane-100. Obviously, there are other factors that play a role in the insect residue adhesion process, for example surface hardness is likely a contributing factor with greater amounts of SMA likely resulting in a softer surface. A softer surface would deform more under direct impact and possibly allow for more wetting to occur. Based on these initial results, it was of interest to test these coatings in a larger wind tunnel that would be more representative of actual aircraft flight conditions than that of the benchtop wind tunnel.

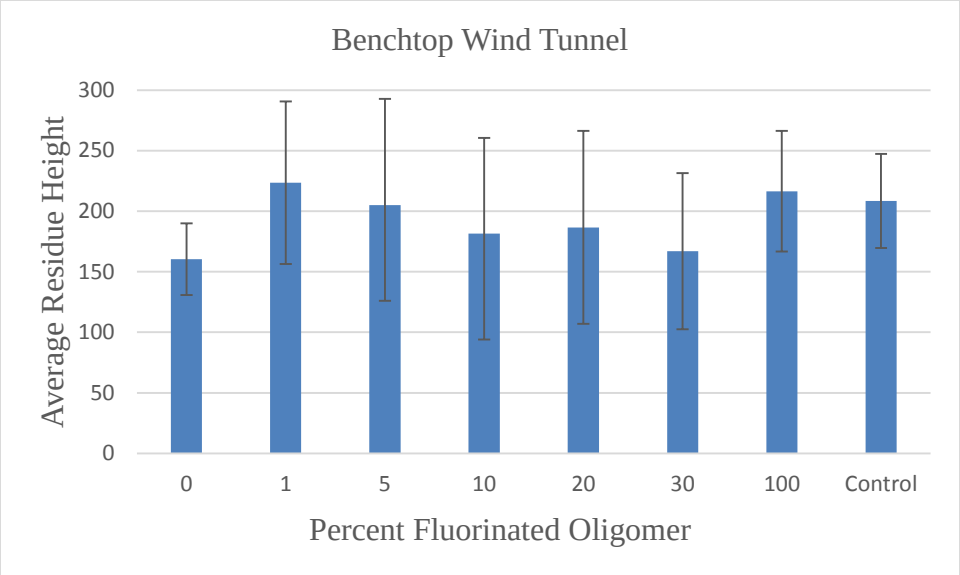


a.

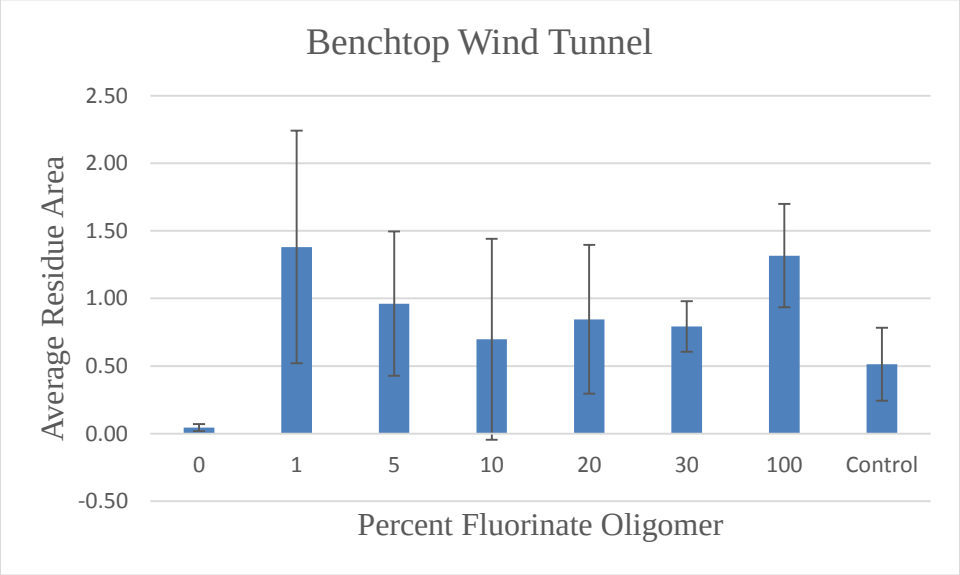


b.

Figure 4.(a) SMA Content vs Average Residue Height For Benchtop Wind Tunnel (b) SMA Content vs Average Residue Areal Coverage For Benchtop Wind Tunnel

**Basic Aerodynamic Research Tunnel (BART) Tests.** Urethanes 0, 10, and 20 were selected to be tested in the BART wind tunnel. Just as with the benchtop wind tunnel, a high speed camera was used to ensure that only whole bug impacts were counted in the analysis of total insect strikes. The high speed camera was also used to investigate the number of strikes with visible residue compared to the number of bug strikes that left little to no visible residue (Table 4). One major difference between the benchtop wind tunnel and the BART wind tunnel is the nature of the insect impacts. The benchtop wind tunnel produced mostly direct impact strikes in which the importance of surface hardness is likely more significant than in a glancing type of impact. The BART wind tunnel more closely emulates the aerodynamics that would be encountered by an aircraft at take-off and landing. In the BART wind tunnel testing, around 30 insects were simultaneously introduced into the airflow resulting in a combination of impact scenarios, both direct and glancing as well as insects that missed the airfoil entirely. The amount of residue left on the coating from the glancing strikes seemed to vary based on the perceived angle of impact and the coating composition. With the use of the high speed camera, it was not uncommon to observe a glancing insect leave an initial residue that then partially released from the surface as the air flow pushed the residue off the surface. Some insects struck the coating surface leaving no visible residues. Table 4 shows the total number of insect strikes captured with high speed photography compared to those that were visible on the surface upon inspection at the completion of the wind tunnel experiment. Urethane-10 had the lowest percentage of visual residues, while having the highest number of insect strikes. This suggests that this coating prevented adhesion of the insect residue to a greater degree than the rest of the coatings under these test conditions.

Table 4. Insect Residue Strike Count for the BART Wind Tunnel Testing

| Coating | Total Strikes Observed on High Speed Photography | Strikes with Visible Residue | Visible Residue % |
|---|---|---|---|
| Urethane-0 | 33 | 19 | 57 |
| Urethane-10 | 37 | 16 | 43 |
| Urethane-20 | 27 | 16 | 59 |
| Control | 21 | 21 | 100 |

A comparison of the data for the coatings tested in the benchtop wind tunnel and the 3 coatings that were tested in the BART wind tunnel along with the control are presented in Figure 5. The coatings as well as the control tested in BART showed lower insect residue height and areal coverage compared to those tested in the benchtop wind tunnel. In the BART test, Urethane-10 exhibited a significantly lower average residue height and areal coverage than the control and the other urethane coatings. This is interesting because in the benchtop wind tunnel, it was Urethane-0 that exhibited the lower residue height and areal coverage. It could be implied that when both direct and glancing strikes occurred on the Urethane-0 coating, more visible residue were left behind from glancing strikes on the coating surface. When tested in the BART wind tunnel, both Urethane-10 and Urethane-20 exhibited lower insect residue areal coverage. Insect residue height was similar for Urethane-0 and 20.

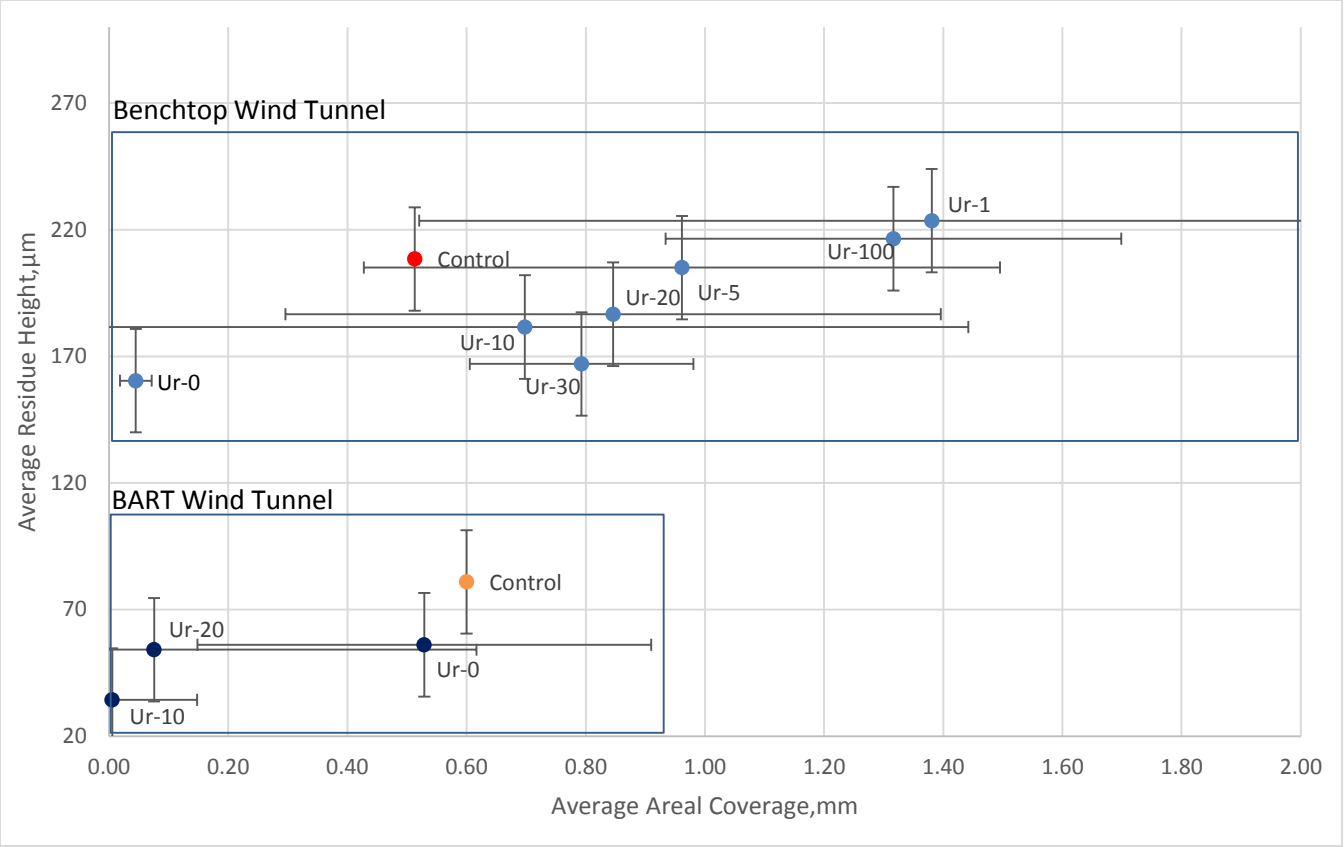


Figure 5. Scatter Plot of Co-Oligomer Coatings Tested in Benchtop Wind Tunnel and in BART Wind Tunnel

In the BART wind tunnel tests, the effect of SMA content in the urethanes seemed to follow the same trend seen in the benchtop wind tunnel testing. The coating with 10% SMA (Urethane-10) has both a lower residual height (Figure 6a) and areal coverage (Figure 6b) than Urethane-20 which contains 20% of the SMA. Both coatings outperformed the control panel. The airfoil used in the BART wind tunnel tests better simulates natural airflow (although not designed for laminar flow) over an airplane wing and resulted in a number of glancing insect strikes. The response of the coating to glancing strikes was markedly different compared to direct impacts indicating that surface hardness may not be as important under these conditions. Thus, the results showed significant reductions in insect residue height and areal coverage on the surface of the coatings.

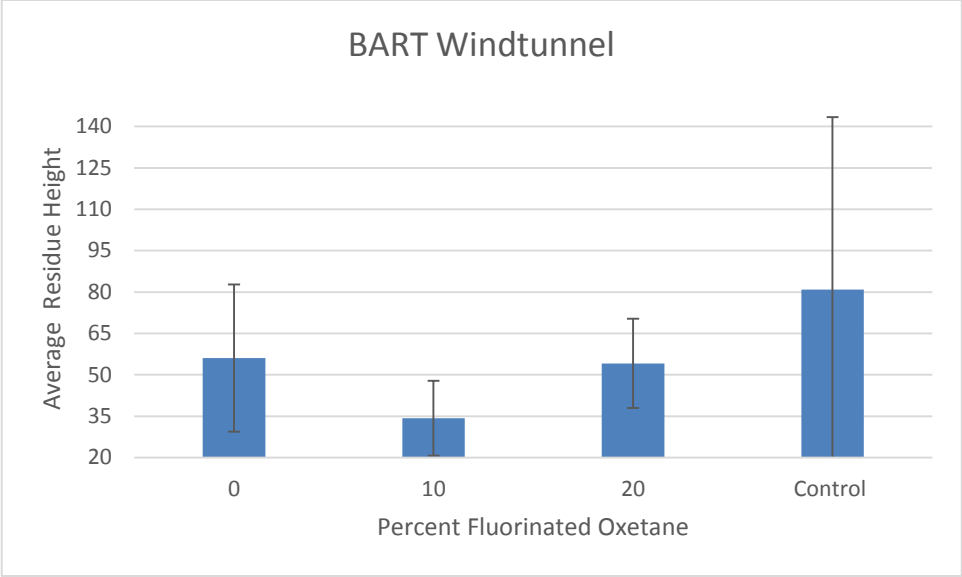


a.

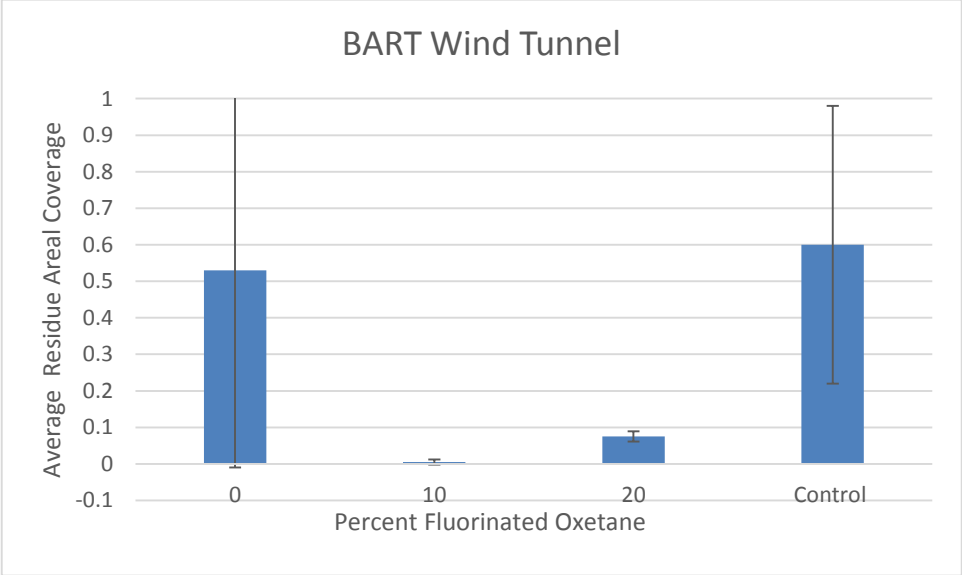


b.

Figure 6.(a) SMA Content vs Average Residue Height for BART Wind Tunnel (b) SMA Content vs Average Residue Areal Coverage for BART Wind Tunnel

**Conclusion.** A series of controlled molecular weight random urethane co-oligomers containing various amounts of a fluorine containing SMA were prepared and characterized. The urethane co-oligomers exhibited advancing water contact angles higher than that of the control. EDS conducted on coatings of these materials indicated that the fluorine content was enriched at the surface and that it was randomly distributed. Some of urethane co-oligomer coatings displayed a resistance to insect residue adhesion compared to the control in small and medium scale wind tunnel tests. However, there was no direct correlation between the insect residue heights and areal coverage and amount of fluorine containing SMA. In comparing results of coatings that were subjected to both wind tunnel tests, there was a significant difference in the insect adhesion residue heights and areal coverage. Clearly, factors other than surface energy can influence the coating behavior including type of impact (direct or glancing), parameters used to assess performance (residue height and aerial coverage) and hardness of coating.

References


[1] C. Wohl, J. Connell, Y. Lin, M. Belcher and F. Palmieri, "Generation and Evaluation of Lunar Dust Adhesion Mitigating Materials," in *AIAA Atmospheric Space Environments Conference*, Honolulu, 2011.

[2] J. Smith, C. Wohl, R. Kreeger, K. Hadley and N. McDougall, "Hydrogen-Bonding Surfaces for Ice Mitigation," NASA/TM–2014-218291, 2014.

[3] C. Wohl, J. Smith, R. Penner, T. Lorenzi and C. S. E. Lovell, "Evaluation of Commercially Available Materials to Mitigate Insect Residue Adhesion on Wing Leading Edge Surfaces," *Progress in Organic Coatings,* vol. 76, pp. 42-50, 2013.

[4] J. Sacristan, C. Mijangos, H. Reinecke, S. Spells and J. Yarwood, "Selective Surface Modification of PVC Films As Revealed by Confocal Raman Microspectroscopy," *Macromolecules ,* vol. 33, pp. 6134-6139, 2000.

[5] V. Kuotsos, E. van der Vegte, P. Grim and G. Hadziioannou, "Isolated Polymer Chains via Mixed Self-Assembled Monolayers:Morphology and Friction Studied by Scanning Force Microscopy," *Macromolecules ,* vol. 31, pp. 116-123, 1998.

[6] A. Janorkar, A. Metters and D. Hirt, "Isolated Polymer Chains via Mixed Self-Assembled Monolayers:Morphology and Friction Studied by Scanning Force Microscopy Surface-Confined Photografting and Increased Degradation Rate Due to an Artifact of the Photografting Process," *Macromolecules ,* vol. 37, pp. 9151-9159, 2004.

[7] D. Cho, Y. Kim and C. Erkey, "Deposition of Block Copolymer Thin Films onto Polymeric Substrates by Adsorption from Supercritical Carbon Dioxide," *Macromolecules,* vol. 38, pp. 1829-1836, 2005.

[8] R. Jahangir, C. McCloskey, W. Mc Clung, R. Labow, J. Brash and J. Santerre, "The Influence of Protein Adsorption and Surface Modifying Macromolecules on the Hydrolytic Degradation of a Poly(ether–urethane) by Cholesterol Esterase," *Biomaterials,* vol. 24, pp. 121-130, 2003.

[9] M. Lopez-Donaire and J. Santerre, "Surface Modifying Oligomers Used to Functionalize Polymeric Surfaces: Consideration of Blood Contact Applications," *J. APPL. POLYM. SCI,* vol. 131, p. 40328, 2014.

[10] H. Sundaram, Y. Cho, M. Dimitriou, J. Finaly, G. Cone, S. Willams, D. Handlin, J. Gatto, M. Callow, J. Callow, E. Kramer and C. Ober, "Fluorinated Amphiphilic Polymers and Their Blends for Fouling-Release Applications: The Benefits of a Triblock Copolymer Surface," *ACS. Appl. Mater. Interfaces ,* vol. 3, p. 3366–3374, 2011.

[11] P. Game, D. Sage and J. Chapel, "Surface Mobility of Polyurethane Networks Containing Fluorinated Amphiphilic Reactive Additives," *Macromolecules ,* vol. 35, pp. 917-923, 2002.

[12] W. Zhang, Y. Zheng, L. Orsini, A. Morelli, G. Galli, E. Chiellini, E. Carpenter and K. Wynne, "More Fluorous Surface Modifier Makes it Less Oleophobic: Fluorinated Siloxane Copolymer/PDMS Coatings," *Langmuir,* vol. 26, no. 8, p. 5848–5855, 2009.

[13] P. Majumdar and D. Webster, "Preparation of Siloxane-Urethane Coatings Having Spontaneously Formed Stable Biphasic Microtopographical Surfaces," *Macromlecules ,* vol. 38, pp. 5857-5859, 2005.

[14] C. J. Wohl, B. M. A. S. Ghose and J. Connell, "Modification of the Surface Properties of Polyimide Films Using Poss Deposition and Oxgen Plasma Exposure," *Appl. Surf. Sci.,* vol. 255, pp. 8135 - 8144, 2009.

[15] Wohl, C.J.; Applin, S. I.; Cooper, L.I.; Connell, J.W., "Copolyimide Surface Modifying Agents for Particle Adhesion Mitigation," in *242nd American Chemical Society National Meeting and Exposition*, Denver, CO, 2011.

[16] R. Zhou, D. Lu, Y. Jiang and Q. Li, "Mechanical Properties and Erosion Wear Resistance of Polyurethane Matrix Composites," *Wear,* vol. 259, pp. 676–683, 2005.

[17] R. A. M. N. U. Gogoi, "Effect of Soft Segment Chain Length on Tailoring the Properties of Isocyanate Terminated Polyurethane Prepolymer, a Base Material From Polyurethane Bandage," *International Journal of Research in Engineering and Technology,* pp. 395-398, 2013.

[18] Y. Tang, J. Santerre, R. Labow and D. Taylor, "Synthesis of Surface-Modifying Macromolecules for use in Segmented Polyurethanes," *J. Appl. Polym. Sci.,* vol. 62, pp. 1133-1145, 1996.

[19] K. Wynne, U. Makal, P. Kurt and L. Gamble, "Model Fluorous Polyurethane Surface Modifiers Having Co-polyoxetane Soft Blocks with Trifluoroethoxymethyl and Bromomethyl Side Chains," *Langmuir,* vol. 23, pp. 10573-1580, 2007.

[20] A. Gregorova, "Application of Differential Scanning Calorimetry to the Characterization of Biopolymers," in *Applications of Calorimetry in a Wide Context - Differential Scanning Calorimetry, Isothermal Titration Calorimetry and Microcalorimetry*, InTech, 2013, pp. 3-20.

[21] E. Siochi, C. Wohl, J. Smith, J. Gardner, R. Penner and J. Connell, "Engineered Surface for Mitigation of Insect Residue Adhesion," in *SAMPE Spring Conference*, Long Beach, CA , 2013.

[22] R. Joslin, "Overview of Laminar Flow Control," NASA/TP-1998-208705, 1998.

[23] W. Sellers and S. Kjelgaard, "The Basic Aerodynamics Research Tunnel-A Facility Dedicated to Code Validation," *AIAA,* vol. 88, pp. 22-33, 1997.

[24] D. Neuhart, L. Jenkins, M. Choudhari and M. Khorrami, "Measurement of the Flowfield Interaction between Tandem Cylinders," *AIAA,* pp. 1-18, 2009.

[25] C. Brunnette, S. Hsu and W. MacKnight, "Hydrogen-Bonding Properties of Hard-Segment Model," *Macromolecules,* vol. 15, pp. 71-77, 1982.

[26] A. Kannan, N. Choudhurry and N. Dutta, "Fluoro-silsesquioxane-urethane Hybrid for Thin Film Applications," *ACS APPL MATER INTER,* vol. 1, pp. 336-347, 2009.

[27] P. Game and D. C. J. Sage, "Surface Mobility of Polyurethane Networks Containing Fluorinated Amphiphilic Reactive Additives," *Macromolecules,* vol. 35, pp. 917-923, 2002.

[28] C.-M. Chang, "Polymer Surface: Modification and Analysis," in *Polymer Surface Modification and Charactrization*, 1994, pp. 1-34.